Pervaporation of Methanol/Dimethyl Carbonate Using SiO_2 Membranes with Nano-Tuned Pore Sizes and Surface Chemistry

Toshinori Tsuru, Akifumi Sasaki, Masakoto Kanezashi, and Tomohisa Yoshioka
Dept. of Chemical Engineering, Hiroshima University, Higashi-Hiroshima, 739-8527, Japan

DOI 10.1002/aic.12436
Published online November 2, 2010 in Wiley Online Library (wileyonlinelibrary.com).

Porous silica membranes with different pore sizes (average pore size: 0.3–1.2 nm) and surface chemistry were prepared from SiO_2, steam-treated SiO_2, SiO_2—ZrO_2, and SiO_2—TiO_2 by sol-gel processing, and were applied to the pervaporation (PV) separation of methanol (MeOH) /dimethyl carbonate (DMC) mixtures at 50°C. Although SiO_2—ZrO_2 membranes demonstrated a separation factor of <10, the SiO_2 porous membranes had an increased separation factor from 10–160. Silica membranes with an average pore size of 0.3 nm showed the highest permselectivity of methanol with a separation factor of 140 and a methanol flux of 180 mol/(m^2h) for MeOH 50 mol% at 50°C. To characterize the surface property of SiO_2 membranes, SiO_2 powdered samples were used for an adsorption experiment of vapor (MeOH, DMC) in single and mixed systems, revealing increased MeOH selective adsorption for SiO_2 powders with hydrophilic and small pores, which was consistent with PV performance. © 2010 American Institute of Chemical Engineers *AIChE J,* 57: 2079–2089, 2011
Keywords: silica membrane, methanol/dimethyl carbonate, pervaporation, adsorption

Introduction

Dimethyl carbonate (DMC) is an environmentally friendly chemical with nontoxicity and quick biodegradation. It has been widely used on a large scale as a precursor for polycarbonate resins and as an electrolyte for lithium-ion cells, the demand for which have increased rapidly.[1,2] DMC is produced by two major processes: phosgenation and carbonylation of methanol. In the carbonylation process, which does not use phosgene and is environmentally friendly, methanol is catalytically oxidatively carbonyled with carbon monoxide and oxygen in a liquid-phase oxidation. Another process for DMC production is the ester-exchange reaction of ethylene carbonate with methanol. In both production processes, DMC must be separated after the reaction from the mixture of methanol (MeOH.) DMC is a raw material for production of diphenyl carbonate (DPC), which is used for the production of a polycarbonate resin. In the production of DPC, DMC reacts with phenol in an esterification reaction, and produces DPC and MeOH. The equilibrium conversion is low—in the range of 10^{-3}–10^{-4}—in ordinal reaction conditions, and, therefore, MeOH must be removed from the reaction mixture to shift the conversion.[2] DMC is often involved with processes mixed with MeOH, and, therefore, must be separated from the mixtures. However, DMC and MeOH form an azeotrope at a methanol concentration of 85 mol% under the total pressure of at 101.3 kPa and are separated using high-pressure distillation, azeotropic-distillation, and adsorption, which require a large amount of energy for separation. So membrane separation, which has been successfully applied to a wide variety of mixtures, including water treatment and dehydration of bioethanols, was expected to be applicable. Pervaporation (PV) holds particular promise for separation at azeotropic points or for mixtures with close boiling points.[3–5]

Although the separation of DMC/MeOH mixtures is quite important, only a limited number of papers have focused on

Correspondence concerning this article should be addressed to T. Tsuru at tsuru@hiroshima-u.ac.jp.

Table 1. List of Membranes Used in This Study

Membrane[a]	material	Firing temperature [°C]	Average pore size[b][nm]	N_2 Permeance[c][mol/(m^2 s Pa)]
SZ-0.5C550	SiO_2-ZrO_2 (Si/Zr = 1/1)	550	0.5	6.8×10^{-8}
SZ-0.6C550	SiO_2-ZrO_2 (Si/Zr = 1/1)	550	0.6	4.60×10^{-6}
SZ-1.2C550	SiO_2-ZrO_2 (Si/Zr = 1/1)	550	1.2	3.30×10^{-6}
ST-0.6C500	SiO_2-TiO_2 (Si/Ti = 3/1)	550	0.6	8.00×10^{-7}
S-0.6C500	SiO_2	500	0.6	1.30×10^{-7}
S-1.0C500	SiO_2	500	1	2.40×10^{-6}
S-0.3C350	SiO_2	350	0.3	1.20×10^{-6}
S-0.4C350	SiO_2	350	0.4	2.00×10^{-6}
S-0.6C350	SiO_2	350	0.6	1.20×10^{-6}
S-0.7C350	SiO_2	350	0.7	4.10×10^{-6}
S-0.7C350ST[d]	SiO_2	350	0.4	3.00×10^{-7}
S-0.4C250	SiO_2	250	0.4	9.00×10^{-8}

[a]Membranes were coded as $$-###C%%% where $$, ###, and %%% indicate membrane materials (SZ:SiO_2ZrO_2, ST:SiO_2—TiO_2, S:SiO_2), average pore sizes, and firing temperatures, respectively.
[b]Determined at 50% of dimensionless permeance by Nanopermporometry.
[c]Measured at 200°C.
[d]With steam treatment (3 days at 80°C and 60% RH).

it. Since MeOH is more hydrophilic and smaller in molecular size than DMC, the strategy for membrane preparation is to use hydrophilic polymers such as chitosan, polyacrylic acid (PAA), and polyvinyl alcohol (PVA).[6–9] Hydrophilic polymeric membranes, including cross-linked chitosan[7] and poly(PAA/PVA) blend membranes,[8] reportedly show MeOH permselectivity over DMC and are capable of breaking azeotropes. Recently, improved performance of chitosan membranes was reported by incorporating inorganic materials such as silica[10] and silicotungstic acid hydrate[11] in the expectation of a greater affinity for MeOH. This new type of organic/inorganic hybrid membranes showed an improved flux in the range of 1 kg/(m^2h) and higher separation factors in the range of 40–50 for MeOH/DMC mixtures.[11]

Inorganic membranes have excellent stability against organic solvents,[12,13] and show high flux and separation factors. Various types of zeolite membranes, such as NaA, NaY, and MFI, have been developed[3,4] and commercialized for the dehydration of organic solvents, including ethanol. Kita et al.[14] completed a MeOH/DMC separation using zeolite NaY membranes, and reported high separation factors at 480 with a high flux of 1.5 kg/(m^2h) for the mixture (50 wt % of MeOH). Other classes of inorganic membranes include ceramics such as SiO_2, TiO_2, and ZrO_2 and composites such as SiO_2ZrO_2, all of which have been applied in PV of a wide variety of separation systems.[3,15,16] Organic aqueous mixtures, including the dehydration of ethanol and isopropanol, have been successfully separated using SiO_2, TiO_2, and SiO_2—ZrO_2 membranes. Organic mixtures such as benzene/cyclohexane can also be successfully separated.[17,18] Although use of SiO_2 membranes for PV has been reported for various applications, no article has reported the separation of MeOH/DMC using porous ceramic membranes. Porous ceramic membranes, in particular SiO_2 membranes, impart great advantage with the ability to tune pore sizes to a similar surface chemistry, because pore sizes of SiO_2 can be controlled by choosing colloidal sols appropriate for coating the separation top layer.[13,15,19] It should be noted that zeolites have specific pore structures (pore size) and surface chemistry, such as the Si/Al ratio, that is, hydrophilicity and hydrophobicity, which makes it difficult to control the pore size of zeolite membranes independent of the Si/Al ratio—hydrophilicity/hydrophobicity.

The purpose of this study was to propose a strategy for MeOH/DMC separation using porous, highly permselective, ceramic membranes. In this work, silica membranes with tuned pore sizes in the range of 0.3–1.2 nm and controlled surface chemistry (hydrophilicity/hydrophobicity) were prepared from SiO_2, SiO_2—ZrO_2, and SiO_2—TiO_2 on porous α-alumina supports by sol-gel processing, and were applied to the PV separation of MeOH/DMC mixtures at 50°C. SiO_2 membranes with and without steam treatment were examined to discuss the effect of hydrophilicity. To characterize the surface properties of SiO_2 membranes, some powdered samples, prepared from colloidal sols by firing at specific temperatures, were used for an adsorption experiment of vapor (MeOH, DMC)—both single and in mixture.

Experimental

Preparation of sols and membranes

The SiO_2 sols were prepared by hydrolysis reaction of tetraethoxysilicate (TEOS) with water using nitric acid as a catalyst, followed by a condensation reaction at the boiling point of sol solutions for 12 h for complete hydrolysis reaction under TEOS concentrations maintained at 2, 1, and 0.5 wt %. Colloidal sizes were successfully controlled in the range of several–100 nm by TEOS concentration. SiO_2—ZrO_2 and SiO_2—TiO_2 colloidal sols were prepared by mixing zirconium tetrabutoxide and titanium tetrapropoxide with TEOS in molar ratios of Si/Zr = 1/1 and Si/Ti, respectively, for the hydrolysis reaction. Cylindrical α-alumina microfiltration membranes (pore size: 1 μm, outer diameter: 10 mm, inner diameter: 8 mm) were used as substrates. After α-alumina powders (200 nm in size; Sumitomo Chemical Corp., Japan), which were mixed with silica sols as a binder, were deposited, silica sols of different colloidal sizes were coated and fired at 250–550°C from larger to smaller colloidal sizes. This coating and firing process for each sol was repeated several times to form a homogeneous separation layer. Some SiO_2 membranes were steam-treated at 80°C and 60% RH for 3 days to make the surface hydrophilic. The preparation of silica sols and membranes has been described in detail in our previous articles.[13,15,16,20,21] Table 1 shows the list of ceramic membranes used in this study. Pore sizes of porous membranes were evaluated using nanopermporometry

Table 2. Properties of Methanol and Dimethyl Carbonate

	Methanol (MeOH)			Dimethyl carbonate (DMC)		
Chemical formula				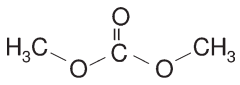		
Molecular weight (MW) [g/mol]	32.04			90.08		
Boiling point [°C]	64.5			90.5		
Liquid density [g/cm^3]	0.7866 (298.15K)			1.0635 (298.15K)		
Antoine Coefficients[a]	A	B	C	A	B	C
	7.19736	1574.99	−34.29	6.4338	1413.0	−44.25
Wilson parameter for MeOH + DMC[b]	$\lambda_{12}-\lambda_{11}$ [J/mol]			$\lambda_{21}-\lambda_{22}$ [J/mol]		
	2759.22			1313.06		
Kinetic diameter [nm][c]	0.380			0.47(Acetone) ∼ 0.63(MTBE)		
Solubility parameters[d][MPa$^{-1/2}$]	δ_d	δ_p	δ_h	δ_d	δ_p	δ_h
	15.1	12.3	22.3	15.8	7.5	10.9

[a] $logP_i^s$/kPa = $(A - B)/(T/K+C)$.[23]
[b] Wilson parameters were obtained at 101.3 kPa.[24]
[c] Stockmayer length parameters based on phase-coexistence data.[25] Since no kinetic diameter for DMC is available, acetone (MW 58.08) and methy tert-butyl ether (MTBE; MW 88.15) were tabulated.
[d] Hansen parameters. δ_d: dispersion, δ_p: polarity, δ_h: hydrogen bonding.[8]

(Nano-Permporometer, Seika Sangyo, Japan); the principle of nanopermporometry is based on the capillary condensation of vapor and the permeation blocking of noncondensable gas such as N_2. Water vapor was used for condensable vapors.[22]

PV measurement

Table 2 summarizes the physicochemical properties of MeOH and DMC used for PV experiments.[8,23–25] The molecular size of MeOH was reported to be 0.38 nm,[25] and no molecular size was available for DMC. Based on the molecular size of acetone (0.47 nm) and methy-tert-butyl-ether (0.63 nm),[25] which consist of similar molecular structures as ketone and ether groups, the molecular size of DMC can be assumed to be larger than that of MeOH. The Hansen solubility parameters of dispersion, and the polar and hydrogen bonding of MeOH are 15.1, 12.3, and 22.3, respectively, whereas those of DMC are 15.5, 3.9, and 9.7, which indicates that MeOH molecules are more hydrophilic and polar.[8]

A schematic diagram of the PV apparatus is shown in Figure 1. Mixtures of methanol (MeOH) and DMC were circulated at 1200 rpm via a stirrer to minimize the effect of concentration polarization on the membrane surface. The temperature was maintained at 50 ± 0.2°C. The pressure on the feed side was maintained at atmospheric pressure, whereas the permeate side was evacuated to nearly 0 kPa using a vacuum pump. The permeate was collected using a liquid nitrogen cold trap during a predetermined time interval. The concentration in the feed was controlled by the periodic addition of MeOH and DMC to the feed. The compositions of the permeate and feed streams were determined using gas chromatography (GC-14B, Shimadzu, Japan).

The separation factor was defined as follows.

$$\alpha = \frac{(y_{\mathrm{MeOH}}/y_{\mathrm{DMC}})}{(x_{\mathrm{MeOH}}/x_{\mathrm{DMC}})} , \quad (1)$$

where x_{MeOH}, x_{DMC}, y_{MeOH}, and y_{DMC} denote the mole fraction of methanol and DMC in feed and permeate, respectively. Permeance, P, was calculated using

$$P_i = J_i/(p_{f,i} - p_{p,i}) , \quad (2)$$

where molar flux of the ith component, J_i, was divided by the partial pressure difference of the ith component across a membrane, $(p_{f,i} - p_{p,i})$. Partial pressure of ith component in feed, $p_{f,i}$, was calculated as $p_{f,i} = \gamma_i x_i P_i^{\circ}$ with vapor pressure, P_i°, by Antoine equation,[23] mole fraction, x_i, and activity coefficient, γ_i, by Wilson parameters[24] (shown in Table 1), while a permeate pressure, p_p, was assumed to be zero.

Adsorption measurement

Adsorption measurements in single and mixed systems were carried out using the schematic diagrams shown in Figures 2a and b, respectively. In the single system, a differential thermal/themogravimetric analyzer (DTG-60, Shimadzu,

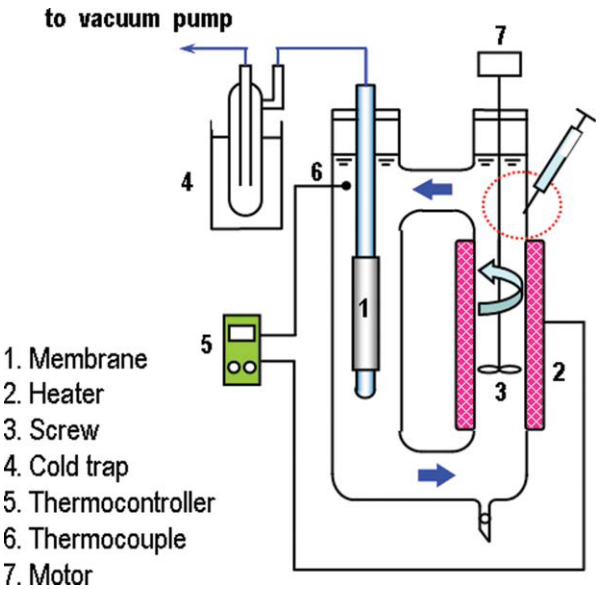

Figure 1. Schematic diagram of PV apparatus

[Color figure can be viewed in the online issue, which is available at wileyonlinelibrary.com.]

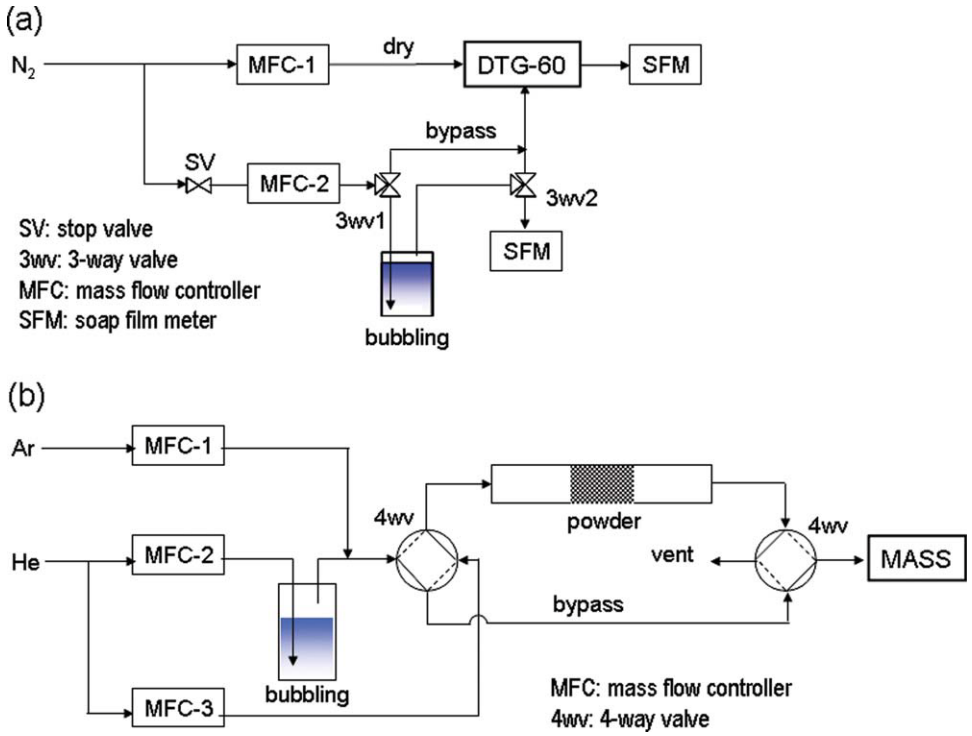

Figure 2. (a). Adsorption measurement for a single system using a differential thermal analysis/thermogravimetry analyzer (DTG-60) (a), and for a binary system using a mass-spectrometer (MASS) (b)

[Color figure can be viewed in the online issue, which is available at wileyonlinelibrary.com.]

Japan) was used for the simultaneous measurement of the weight change (adsorption amount) and the heat flow (heat of adsorption). SiO_2 powders were pretreated at 250–400°C in DTG-60 for 30 min under a dry N_2 flow (MFC-1) to remove adsorbed water. N_2 (MFC-2) was humidified with either MeOH or DMC by bubbling through MeOH or DMC controlled at 10–20°C, and then introduced into the DTG-60. The relative pressure of MeOH or DMC was controlled in a range of 0.01–0.2 by the flow rate of the dry N_2 (MFC-1) and that of humidified N_2 (MFC-2). Figure 2b shows a schematic diagram for the adsorption measurement of binary systems. Silica powders (0.01–0.05 g) packed in the glass tube were first heated at 400°C to remove adsorbed water, and then controlled at 50°C under pure He flow (MFC-3; 4-way vales: solid direction). He (MFC-2, flow rate: 10 ccm) was bubbled through MeOH/DMC (4°C; mole fraction: 0.165/

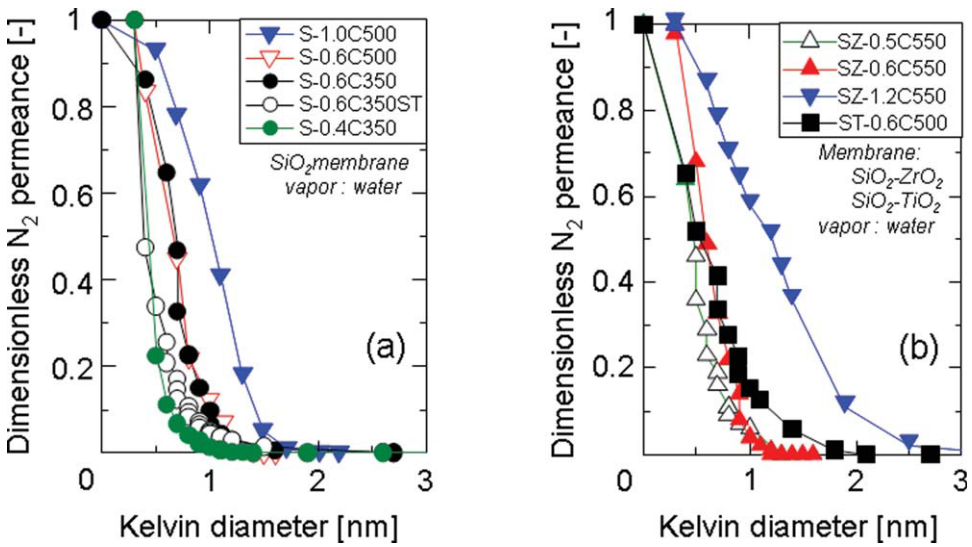

Figure 3. Nanopermporometry characterization of the pore size distribution of SiO_2—ZrO_2 and SiO_2-TiO_2 membranes (a), and SiO_2 membranes (b). (Membrane code numbers are listed in Table 1)

[Color figure can be viewed in the online issue, which is available at wileyonlinelibrary.com.]

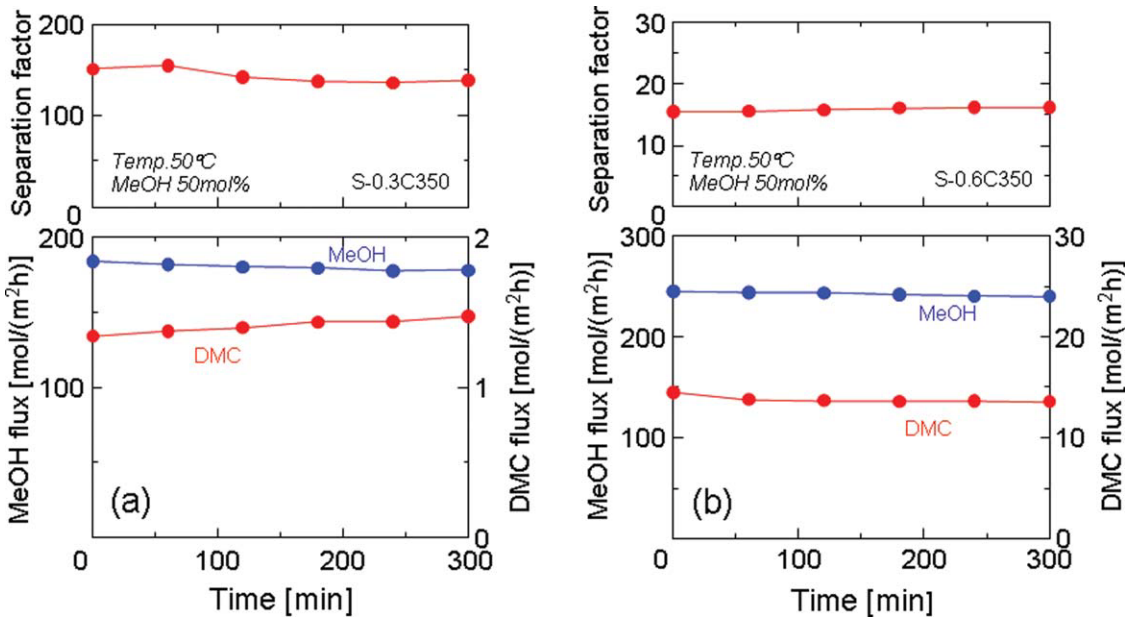

Figure 4. Time course of PV performance for MeOH/DMC = 0.5/0.5 (molar ratio) at 50°C using silica membranes with different pore sizes of 0.3 nm (S-0.3C350) (a), and 0.6 nm (S-0.6C350) (b) (firing temperature 350°C; membrane code-numbers are listed in Table 1).

[Color figure can be viewed in the online issue, which is available at wileyonlinelibrary.com.]

0.835), and mixed with a small amount of Ar (MFC-1, 0.5 ccm) as a calibration gas, and was confirmed by a mass-spectrometer (MASS, Shimadzu Corp., Japan) to be in a steady state. By simultaneously changing two 4-way valves (from solid to dotted direction), MeOH/DMC vapor was introduced to the sample, and the break-through curves were monitored by MASS. The vapor pressure of MeOH and DMC introduced to the sample was controlled to 3 kPa by the temperature of a water bath.

Result and Discussion

Characterization of porous ceramic membranes

Figures 3a and b show the dimensionless N_2 permeance normalized by dry N_2 permeance (Kelvin diameter = 0 nm), as measured by nanopermporometry technique (NanoPerm-Porometer; Seika Sangyo, Japan), of five SiO_2 membranes, and SiO_2—ZrO_2 and SiO_2—TiO_2 membranes, respectively. For the nanopermporometry, the nitrogen flux was measured as a function of the relative pressure of water vapor, p, in the feed, which could be converted to a Kelvin diameter, D_K, using the Kelvin equation

$$RT \ \ln(p/p_s) = -4v\sigma\cos\theta/D_K \ , \qquad (3)$$

where p_s, v, and σ are the saturated vapor pressure of water, the molar volume of the condensed vapor, and the surface tension, respectively, and are assumed to be the same as those in bulk. The θ is the contact angle inside the membrane pores, and complete wetting was assumed ($\theta = 0$) for simplicity. Since pores smaller than the corresponding Kelvin diameter were filled with capillary-condensed water and the condensed water blocked the permeation of nitrogen, the dimensionless permeance—or the nitrogen permeance normalized by the pure N_2 permeance—is the permeance ratio through pores unfilled with capillary-condensed water, and the curve corresponds to the pore-size distribution, as with a cut-off curve. Table 2 summarizes the average pore sizes defined at 50% of dimensionless permeance and the nitrogen permeance (dry). The average pore sizes of SiO_2, SiO_2—ZrO_2, and SiO_2—TiO_2 membranes were successfully controlled in a range from 0.4 to 1.0 nm by choosing sols of appropriate colloidal sol diameters and by controlling the firing temperatures during the final coating step. Membrane S-0.7C350ST, which was prepared by firing a SiO_2 membrane at 350°C (S-0.7C350), with the subsequent steam-treatment, showed an average pore size of 0.4 nm, which was smaller than S-0.7C350, that is, a SiO_2 membrane fired at 350°C without steam-treatment. This was probably due to the generation of silanol groups by steam treatment. Although inorganic membranes are considered to be stable to solvents, this is not always true for surface chemistry. The surface of silica is subject to hydrolysis, that is, siloxane bonding reacts with water and generates silanol groups in both the gas and liquid phases, resulting in a reduced pore size and increased hydrophilicity.[13,15,20,26] This phenomena has been confirmed with CVD[27] and carbonized-template silica[28] membranes.

PV performance of porous ceramic membranes

The separation mechanism through porous membranes can be ascribed to the molecular sieving and the affinity between permeating molecules and membranes. As shown in Table 2, MeOH is more polar and hydrophilic than DMC, and a smaller molecule than DMC. Figures 4a and b show the time courses of two silica membranes with average pores of 0.3 and 0.6 nm, respectively. The pore sizes of the two SiO_2 membranes, which were fired at 350°C, were controlled

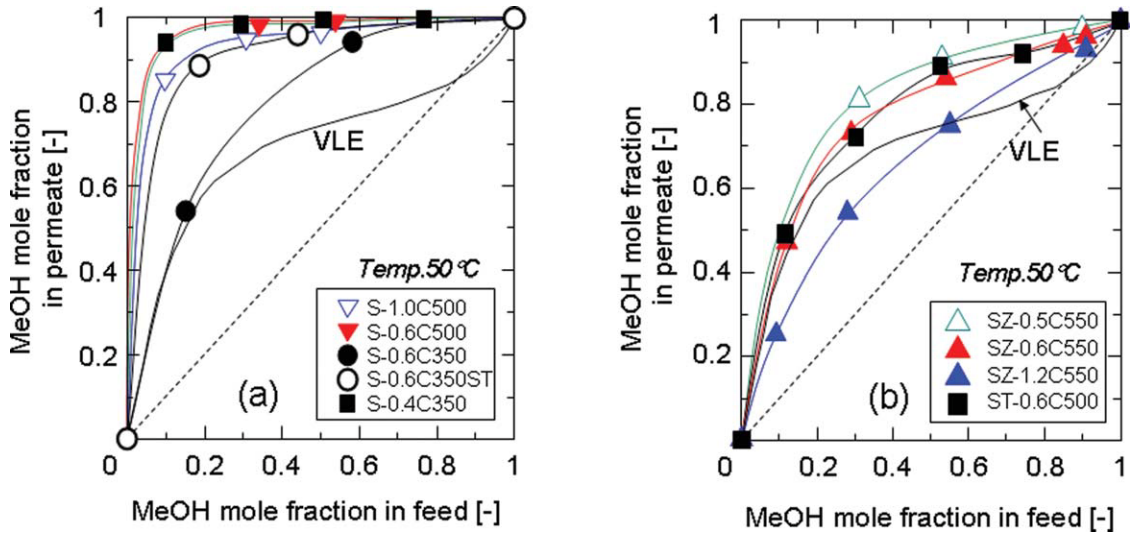

Figure 5. PV performance of SiO_2 (a) and SiO_2—ZrO_2 and SiO_2—TiO_2 (b) membranes. (VLE: vapor-liquid equilibrium; membrane code-numbers are listed in Table 1)

[Color figure can be viewed in the online issue, which is available at wileyonlinelibrary.com.]

using different sizes of coating sols. Silica membranes with pore sizes of 0.3 nm (S-0.3C350) and 0.6 nm (S-0.6C350) showed separation factors of 140 and 15 with methanol flux of 180 and 240 mol/(m^2 h), respectively, for MeOH/DMC of 0.5/0.5 (molar ratio) at 50°C. High flux and separation factors were obtained by S-0.3C350. Separation factor increased with smaller pore sizes, suggesting a significance of the molecular sieving effect. Interestingly, all silica membranes show approximately constant PV performance (separation factors, MeOH flux) as a function of time.

Figures 5a and b summarize the PV performances of SiO_2, SiO_2—ZrO_2 and SiO_2—TiO_2 membranes with pore sizes in the range of 0.4 to 1.2 nm. All ceramic membranes showed perm-selectivity to MeOH over DMC even at the azeotropic point of 86 mol% MeOH. SiO_2 membranes, which are shown in Figure 5a, clearly demonstrate higher separation ability compared with the SiO_2—ZrO_2 and SiO_2—TiO_2 membranes shown in Figure 5b. It should be noted that contact angle, θ, which was assumed to be zero in Eq. 3, is dependent on the types of materials and possibly on the firing conditions even for the same materials due to the dehydration of surface hydroxyl groups such as silanol groups. Therefore, a comparison of pore sizes should be discussed for the same materials and for the same firing conditions. However, distinct differences between SiO_2 and SiO_2—ZrO_2 strongly suggest that surface chemistry plays an important role in determining separation ability. Another point that should be addressed is the molecular sieving effect. Membranes prepared at the same firing temperature, which correspond to a similar surface chemistry, show higher separation performance for both SiO_2 and SiO_2—ZrO_2 membranes with smaller pore sizes. Since the molecular size of MeOH is smaller

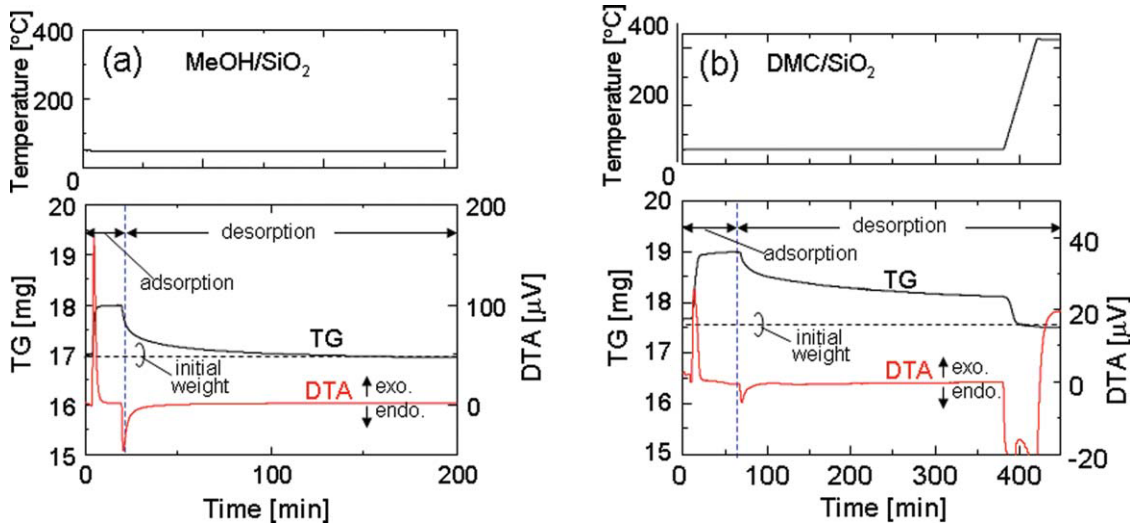

Figure 6. Time course of differential thermal analysis (DTA) and thermogravimetry (TG) signals during adsorption and desorption to silica powders.

[Color figure can be viewed in the online issue, which is available at wileyonlinelibrary.com.]

Table 3. Adsorption Properties of Single Components

Samples	Materials (firing temperature)	D_p[a] [nm]	S_{BET}[a] [m^2/g]	Adsorption [mmol/g]			Ratio of desorption to adsorption[d]	
				MeOH[b]	DMC[c]	MeOH/DMC	MeOH	DMC
P-S500-1.8	SiO_2(500)	1.8	590	1.78	0.86	2.1	0.95	0.77
P-S500ST-2.0	SiO_2ST(500)	2.0	510	1.31	0.70	1.9	0.93	0.72
P-SZ550-2.4	SiO_2ZrO_2(550)	2.4	30	0.18	0.10	1.8	0.90	0.62

[a]Nitrogen adsorption.
[b]$p/p_s = 0.10$.
[c]$p/p_s = 0.15$.
[d]Desorption at 50°C.

than that of DMC, porous membranes with a smaller pore size and controlled surface chemistry must be realized to achieve excellent PV separation. In conclusion, Figures 5a and b suggest the importance of both surface chemistry and the molecular sieving effect, and this will be examined in the section Preferential adsorption in single and mixed systems.

Preferential adsorption in single and mixed systems

Kita et al.[14] measured the adsorption amount of methanol, benzene, and cyclohexane to zeolite Y powders and found that more adsorptive compounds showed preferential permeation for a zeolite Y membrane. As discussed in previous sections, preferential adsorption is suggested to play an important role in determining PV performance also for amorphous silica membranes. Therefore, it is important to evaluate adsorption properties for powdered samples. Figures 6a and b show the time courses for differential thermal analysis (DTA) and thermogravimetry (TG) signals for MeOH and DMC in single systems, respectively. After introducing vapor to the SiO_2 powder, the TG signal increased for several to 10 min and then reached a steady value, while the DTA signal increased and showed a sharp exothermic peak due to the heat of adsorption. After confirming the steady state—the constant weight of the powdered sample (constant TG signal) and no heat flux (zero DTA signal)—desorption was carried out by bypassing a bubble under the N_2 flow. As shown in Figure 6a, approximately all adsorbed methanol was desorbed after ~100 min of receiving the endothermic heat of desorption. However, DMC was not completely desorbed even after 300 min at 50°C, and ~30% of DMC was still adsorbed onto the silica surface. After heating the sample to 400°C, the sample weight returned to its initial value. The time course indicates that DMC adsorbed both irreversibly and reversibly, and, therefore, the adsorption of DMC was stronger than that of MeOH. Table 3 summarizes the adsorption properties of MeOH and DMC in a single component of silica and silica-zirconia powders: P-S500-1.8 (SiO_2 fired at 500°C; pore size: 1.8 nm; without hydrothermal treatment), P-S500ST-2.0 (hydrothermal treated P-S500-1.8; pore size: 2.0 nm) and P-SZ550-2.4 (SiO_2ZrO_2 fired at 550°C; pore size: 2.4 nm). P-S500ST-2.0 showed a lower surface area due to densification of the silica networks, as discussed previously. The adsorption amount ratios of MeOH to DMC were ~2 for all samples, which is close to the ratio of molar density in liquid phase (MeOH 24.5 kmol/m^3, DMC 11.7 kmol/m^3), suggesting the contribution of capillary condensed vapors is most significant under the present conditions [$p/p_s = 0.1$ (MeOH), 0.15 (DMC)]. Under isothermal conditions, MeOH desorbed higher than 90%, while DMC only desorbed 60–80%, showing strong and irreversible adsorption for DMC.

The heat of adsorption for MeOH and DMC with and without hydrothermal treatment was obtained by integrating the DTA signal shown in Figure 6. SiO_2 powder showed a larger heat of adsorption for DMC (≈66 kJ/mol at $p/p_s \approx 0.1$) than for MeOH (≈56 kJ/mol), although the two molecules have approximately the same heat of evaporation (MeOH: 35.3 kJ/mol, DMC: 38.4 kJ/mol at 298 K). This larger heat of adsorption may be caused by the irreversible

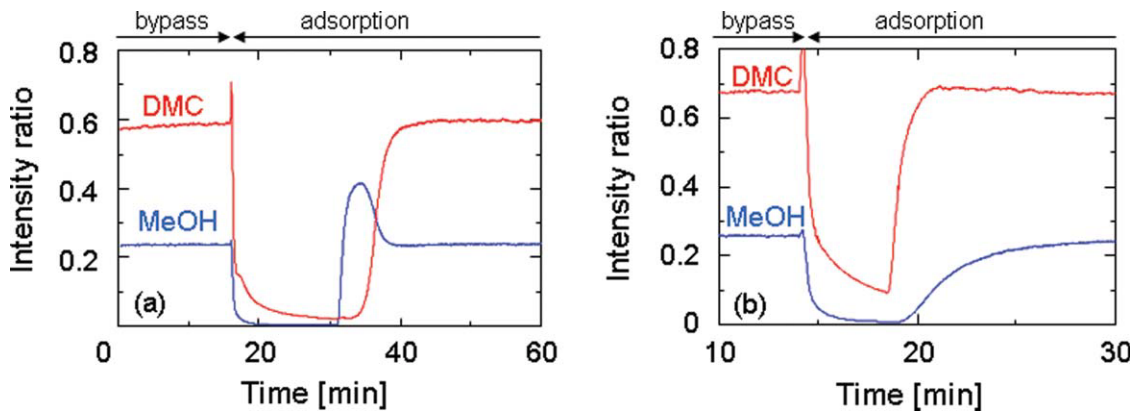

Figure 7. (a) and (b). Time course of the mass intensity ratio of DMC and MeOH to Ar.

(4-way valves in Figure 2 (b) was changed from bypass to adsorption at 16 and 14 min for SiO_2 P-S500ST-2.0 and P-S500ST-0.86, respectively. He and Ar were fed at a constant flow rate of 50 and 0.5 cm^3/min, respectively.) [Color figure can be viewed in the online issue, which is available at wileyonlinelibrary.com.]

Table 4. Adsorption Properties of Silica Powdered Samples for Binary Mixtures

Samples	Materials	D_p[a] [nm]	S_{BET}[a] [m^2/g]	Adsorption[b] mmol/g]		
				MeOH	DMC	MeOH/DMC
P-S500-1.8	SiO_2(500)	1.8	590	0.77	1.43	0.53
P-S500ST-2.0	SiO_2ST(500)[c]	2.0	510	0.95	1.02	0.93
P-S500ST-0.86	SiO_2ST(500)[c]	0.86	99	0.73	0.26	2.8

[a]Nitrogen adsorption.
[b]MeOH, DMC: 3 kPa.
[c]Steam-treatment sil0ica.

adsorption of DMC to the SiO_2 surface, which is consistent with the ratio of desorption to adsorption in Table 3. Hydrothermally treated SiO_2, which had an increased number of silanol groups and hydrophilic surface chemistry, showed a larger heat of adsorption for both MeOH (≈72 kJ/mol) and DMC (≈72 kJ/mol) due to increased interaction with silanol groups (adsorption based on hydrogen bonding) compared with SiO_2 powder without hydrothermal treatment. More importantly, although the heat of adsorption of DMC was larger than that of MeOH for SiO_2 powder without hydrothermal treatment, hydrothermally treated SO_2 showed approximately the same heat of adsorption for both MeOH and DMC due to increased interaction with MeOH.

Figures 7a and b show the break-though curves of the MeOH/DMC binary mixture for SiO_2 powder with and without hydrothermal treatment using mass spectroscopy (MASS). The partial pressures of MeOH and DMC were kept at 3 kPa under He (flow rate: 10 ccm) and Ar (0.5ccm) flow, corresponding to the relative pressures of 0.05 for MeOH and 0.13 for DMC. After confirming a steady MASS intensity, that is, concentration, of MeOH and DMC through bypassing the SiO_2 powders, MeOH/DMC vapor was introduced to the SiO_2 powders at 16 (a) and 14 (b) min to obtain the breakthrough curve. In Figure 7a, both signals decreased approximately to zero, since both MeOH and DMC were adsorbed to the silica powders (P-S500-2.0). At 33 min, MeOH started to increase the MASS signal and showed peak intensity, and then returned to a steady signal, which was approximately the same as the initial intensity. The MASS peak, which was larger than that of the feed vapor, can be ascribed to desorption by DMC. This is a typical adsorption pattern for the binary system, and can be explained due to a difference in affinity or adsorption intensity between vapors and the surface of silica. MeOH vapors adsorbed on SiO_2 at the beginning of the breakthrough experiment were gradually displaced by DMC vapor, which was more adsorptive in the binary vapor and continuously flowed in from the inlet. Therefore, MeOH vapor concentration at 35 min was increased above the inlet concentration. In other words, the more strongly adsorbed adsorbate, DMC, displaced the weaker adsorbate, MeOH. However, in Figure 7b, steam-treated SiO_2 powder (P-S500ST-0.86), which had a smaller pore size (0.86 nm) and a more hydrophilic surface chemistry, showed no peak observed for MeOH, and it took a longer time before the breakthrough of MeOH, indicating that MeOH was more adsorptive than DMC.

By integrating the breakthrough curve, it is possible to obtain binary adsorption, as summarized in Table 4. The SiO_2 powder, P-S500-1.8 (SiO_2, pore size: 1.8 nm, without hydrothermal treatment) showed an MeOH/DMC adsorption ratio of 0.53, and P-S500ST-2.0 (SiO_2, pore size: 2.0 nm, with hydrothermal treatment) showed an adsorption ratio of 0.93. Since the pore sizes were approximately the same, the increased MeOH/DMC adsorption ratio can be ascribed to the hydrophilic surface properties of P-S500ST-2.0 due to the increased hydrophilic and polar nature of MeOH over DMC. P-S500ST-0.86, which had a pore size of 0.86 nm, showed MeOH/DMC adsorption ratio of 2.8, which was larger than P-S500ST-2.0 that was also steam-treated and was supposed to have similar surface properties (hydrophilicity). This comparison suggests that the increased selectivity was due to the molecular sieving effect and to the surface chemistry.

Concentration dependency of PV performance

Figures 8a and b show the concentration dependency of MeOH and DMC permeance for SiO_2—ZrO_2 membranes and

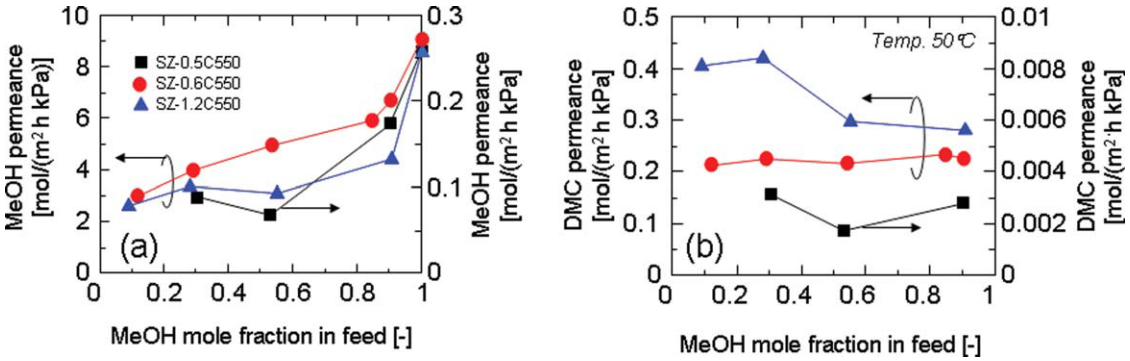

Figure 8. (a) and (b). Concentration dependency of permeance for MeOH (a) and DMC (b) through SiO_2—ZrO_2 membranes with different pore sizes.

(The membrane code numbers are listed in Table 1; arrows in the figures indicate the direction of the left and right axis.) [Color figure can be viewed in the online issue, which is available at wileyonlinelibrary.com.]

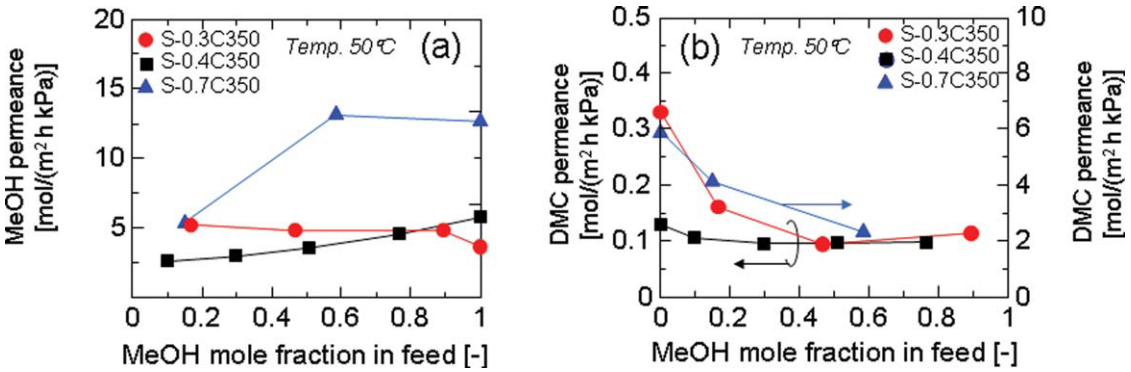

Figure 9. (a) and (b). The concentration dependency of permeance of MeOH (a) and DMC (b) through SiO_2 membranes with different pore sizes.

(The membrane code numbers are listed in Table 1; arrows in the figures indicate the direction of the left and right axis.) [Color figure can be viewed in the online issue, which is available at wileyonlinelibrary.com.]

Figures 9a and b show SiO_2 membranes fired at 350°C. With an increase in MeOH concentration in the feed, MeOH flux increased and DMC flux decreased for both SiO_2 and SiO_2—ZrO_2 membranes. No clear difference was observed in terms of permeate flux. However, permeances, which are normalized fluxes by the pressure difference across a membrane, show an interesting tendency for both MeOH and DMC with SiO_2 and SiO_2—ZrO_2 membranes. As shown in Figures 8a and b, with an increase in MeOH concentration, the permeance of MeOH increased gradually and drastically at low and high MeOH concentrations, respectively, while that of DMC was approximately constant and was not affected by MeOH concentration. This tendency was observed and confirmed with the three different SiO_2—ZrO_2 membranes with different pore sizes from 0.5 to 1.2 nm. However, SiO_2 membranes fired at 350°C showed approximately constant permeance for MeOH, irrespective of MeOH concentration, with a substantial decrease in DMC permeance at low MeOH concentrations. This tendency was the opposite of SiO_2—ZrO_2 membranes.

Considering the molecular characteristics, MeOH is a more hydrophilic, polar, and smaller molecule than DMC, and the adsorption measurements have confirmed that silica powders with hydrophilicity and a small pore size showed preferential separation toward MeOH over DMC. The concentration dependency of permeance through SiO_2 and SiO_2—ZrO_2 membranes can be explained as follows. Porous membranes consist of small pores that allow permeation of only MeOH, and large pores that allow both DMC and MeOH. Since no effect of DMC on MeOH permeance was observed for SiO_2 membranes, SiO_2 membranes can be considered to consist mostly of small pores. However, the DMC that permeated through large pores showed a decreased permeance with increased MeOH concentration, since the hydrophilic surface of SiO_2 allowed preferential adsorption of MeOH and blocked the adsorption and permeation of

Table 5. Comparison of PV Performance for MeOH/DMC Separation Using Organic and Inorganic Membranes, as Reported in the Literature

		MeOH concentration		MeOH flux	DMC flux	Total flux	Total flux	Separation factor	Permeance [mol/(m²hkPa)]	
Membrane code	T [°C]	[mol%]	[wt%]	[mol/m²h]	[mol/m²h]	[mol/m²h]	[kg/m²h]		MeOH	DMC
SZ-0.5C550	50	53	29	3.0	0.28	3.3	0.1	10	0.08	0.019
SZ-0.6C550	50	54	29	220.0	34.80	254.8	10.2	5	5.46	2.451
SZ-1.2C550	50	55	30	140.0	47.30	187.3	8.7	2	3.45	3.365
ST-0.6C500	50	52	28	73.2	8.29	81.5	3.1	8	1.85	0.573
S-0.6C500	50	54	29	3.9	0.03	3.9	0.1	110	0.10	0.002
S-1.0C500	50	50	26	87.6	2.75	90.4	3.1	32	2.25	0.186
S-0.3C350	50	47	24	178.0	1.47	179.5	5.8	137	4.72	0.097
		17	7	102.5	3.21	105.7	3.6	156	5.15	0.162
S-0.4C350	50	51	27	136.3	1.46	137.8	4.5	90	3.47	0.100
		30	13	86.6	1.72	88.3	2.9	117	2.94	0.098
S-0.6C350	50	52	28	240.6	13.58	254.2	8.9	16	6.08	0.938
S-0.7C350	50	58	33	533.6	32.45	566.1	20.0	12	12.84	2.380
S-0.7C350ST	50	45	23	193.4	7.08	200.5	6.8	33	5.23	0.458
S-0.4C250	50	51	27	83.8	0.89	84.7	2.8	91	2.14	0.061
zeolite Y [14]	50	74	50	47.7	0.04	47.7	1.5	480	1.03	0.003
chitosan + APTEOS[10]	50	74	50	37.3	0.34	37.6	1.2	39	0.81	0.030
	50	75	51	35.3	0.29	35.6	1.2	41	0.76	0.027
silicotungstic acid/chitosan[11]	50	55	30	40.2	0.80	41.1	1.4	42	0.99	0.057
	50	55	30	38.0	0.63	38.6	1.3	50	0.94	0.045
PAA/PVA[8]	60	74	50	14.8	0.47	15.3	0.5	12	0.21	0.029

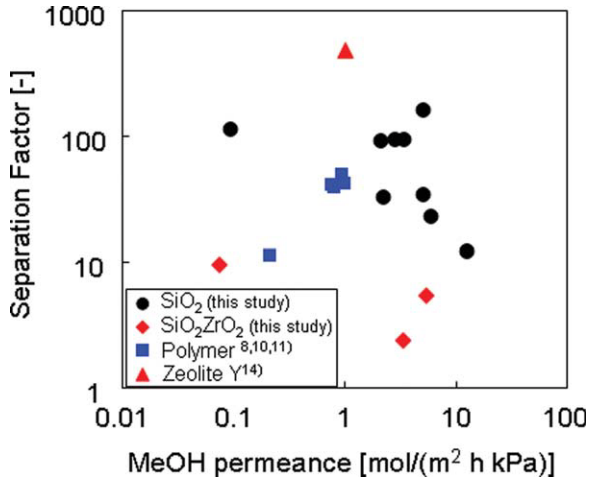

Figure 10. Separation factor as a function of MeOH permeance for SiO_2, SiO_2—ZrO_2, zeolite and polymeric membranes.

[Color figure can be viewed in the online issue, which is available at wileyonlinelibrary.com.]

DMC, and the thickness of adsorbed MeOH increased with MeOH concentration, resulting in decreased DMC permeance. However, SiO_2—ZrO_2 membranes showed increased MeOH permeance and constant DMC permeance against MeOH concentration, suggesting that SiO_2—ZrO_2 membranes consisted of relatively large pores that allowed both MeOH and DMC permeation, and showed preferential adsorption of DMC, which was also consistent with the single and mixed adsorption of MeOH and DMC.

Table 5 summarizes PV performance for MeOH/DMC separation by porous ceramic membranes prepared in this study, along with polymeric membranes and zeolite-Y membranes. Figure 10 shows a trade-off curve between the separation factor and the permeance of MeOH. Since the separation conditions, such as concentration and temperature, are not always the same in the literature, permeance, P, calculated by the same procedure as in Experimental was tabulated for comparison with polymeric and inorganic membranes. It is obvious that SiO_2 membranes showed superior PV performance to SiO_2—ZrO_2 membranes, probably because of increased hydrophilic surface chemistry. Polymeric membranes showed rather low selectivity and flux, whereas zeolite Y membranes showed quite high selectivity and rather low permeate flux. Commercialized inorganic PV membranes for alcohol dehydration, including zeolite A and amorphous SiO_2,[3,29] show a water permeance of 3.7–4.2 and 6.2–8.7 mol/(m^2 h kPa) and separation factors of 3,300–27,000 and 90–120, respectively. SiO_2 membranes in this study showed a MeOH flux higher than 5 mol/(m^2 h kPa) and a separation factor higher than 100, which suggests successful preparation through the control of pore sizes and hydrophilic surface chemistry.

Conclusions

Porous ceramic membranes with a controlled pore size and surface chemistry were prepared for the PV of MeOH/DMC mixtures.

(1) All ceramic membranes, SiO_2, SiO_2—ZrO_2, and SiO_2—TiO_2 (average pore size: 0.3–1.2 nm), showed MeOH permselectivity—even at the azeotropic point.

(2) Separation performance increased with decreased pore sizes of membranes and with increased hydrophilicity.

(3) Although SiO_2—ZrO_2 membranes having controlled average pore sizes from 0.6 to 1.2 nm showed a separation factor of <10, porous SiO_2 membranes were found to show an increased separation factor ranging from 10–160. SiO_2 membrane showed excellent performance (MeOH flux of 180 mol/(m^2 h), separation factor = 140 for MeOH 50 mol%), which was better than either organic or inorganic membranes, including zeolite Y membranes.

(4) Adsorption by both single and mixed systems confirmed that membranes with a hydrophilic surface and controlled pore sizes, as small as MeOH molecules, show possibilities for high permeation and selectivity of MeOH.

Literature Cited

1. Delledonne D, Rivett F, Romano U. Developments in the production and application of dimethylcarbonate. *Appl Catal A*. 2001;221:241–251.
2. Haubrock J. The process of dimethyl carbonate to diphenyl carbonate: thermodynamics, reaction kinetics and conceptual process design, PhD thesis, University of Twente, The Netherlands, ISBN: 90-365-2609-8.
3. Sommer S, Melin T. Performance of microporous inorganic membranes in the dehydration of industrial solvents. *Chem Eng Process*. 2005;44:1138–1156.
4. Wee SL, Tye CT, Bhatia S. Membrane separation process- Pervaporation through zeolite membrane. *Sep Purif Technol*. 2008;63:500–516.
5. Shao P, Huang RYM. Polymeric membrane pervaporation. *J Membr Sci*. 2007;287:162–179.
6. Won W, Feng X, Lawless D. Pervaporation with chitosan membranes: separation of dimethyl carbonate/methanol/water mixtures. *J Membr Sci*. 2002;209:493–508.
7. Won W, Feng X, Lawless D. Separation of dimethyl carbonate/methanol/water mixtures by pervaporation using crosslinked chitosan membranes. *Sep Purif Technol*. 2003;31:129–140.
8. Wang L, Li J, Lin Y, Chen X. Separation of dimethyl carbonate/methanol mixtures by pervaporation with poly(acrylic acid)/ poly(vinyl alcohol) blend membranes. *J Membr Sci*. 2007;305:238–246.
9. Wang L, Li J, Lin Y, Chen X. Crosslinked poly(vinyl alcohol) membranes for separation of dimethyl carbonate/methanol mixtures by pervaporation. *Chem Eng J*. 2009;146:71–78.
10. Chen JH, Liu QL, Fang J, Zhu AM, Zhang QG. Composite hybrid membrane of chitosan-silica in pervaporation separation of MeOH/DMC mixtures. *J Colloid Interface Sci*. 2007;316:580–588.
11. Chen JH, Liu QL, Zhu AM, Zhang QG, Fang J. Pervaporation separation of MeOH/DMC mixtures using STA/CS hybrid membranes. *J Membr Sci*. 2008;315:74–81.
12. Vandezande P, Gevers L, Vankelecom I. Solvent resistant nanofiltration: separating on a molecular level. *Chem Soc Rev*. 2008;37:365–405.
13. Tsuru T. Nano/subnano-tuning of porous ceramic membranes for molecular separation. *J Sol-Gel Sci Technol*. 2008;46:349–361.
14. Kita H, Fuchida K, Horita H, Asamura H, Okamoto K. Preparation of Faujasite membranes and their permeation properties. *Sep Purif Technol* 2004;25:261–268.
15. Yang J, Yoshioka T, Tsuru T, Asaeda M, Pervaporation characteristics of aqueous-organic solutions with microporous SiO_2- ZrO_2 membranes: Experimental study on separation mechanism. *J Membr Sci*. 2006;284:205–213.
16. Asaeda M, Ishida M, Waki T. Pervaporation of aqueous organic acid solutions by porous ceramic membranes. *J Chem Eng Jpn*. 2005;38:336–343.
17. Asaeda MK, Okazaki A. Nakatani. Preparation of thin porous silica membranes for separation of non-aqueous organic solvent mixtures by pervaporation. *Ceram Trans*. 1992;31:411–420.
18. Garcia Villaluenga JP, Tabe-Mohammadi A. A review on the separation of benzene/cyclohexane mixtures by pervaporation processes. *J Membr Sci* 2000;169:159–174.

19. Tsuru T, Izumi S, Yoshioka T, Asaeda M. Temperature effect on transport performance by inorganic nanofiltration membranes. *AIChE J*. 2000;46:565–574.
20. Asaeda M, Yamasaki S. Separation of inorganic/organic gas mixtures by porous silica membranes. *Sep Pur Technol*. 2001;25,151–159.
21. Tsuru T, Yamaguchi K, Yoshioka T, Asaeda M. Methane steam reforming by microporous catalytic membrane reactors. *AIChE J*. 2004;50:2794–2805.
22. Tsuru T, Hino T, Yoshioka T, Asaeda, M. Permporometry characterization of microporous ceramic membranes. *J Membr Sci*. 2001;186:257–265.
23. Fang YJ, Qian JM. Isobaric vapor-liquid equilibria of binary mixtures containing the carbonate group –OCOO-. *J Chem Eng Jpn*. 2005;50:340–343.
24. Rodriguez JC, Dominguez A, Tojo J. Vapor-liquid equilibria of dimethyl carbonate with linear alcohols and estimation of interaction parameters for the UNIFAC and ASOG method. *Fluid Phase Equilib*. 2002;201:187–201.
25. van Leeuwen M. Derivation of Stockmayer potential parameters for polar fluids. *Fluid Phase Equilib*. 1994;99:1–18.
26. Igi R, Yoshioka T, Ikuhara YH, Iwamoto Y, Tsuru T. Characterization of Co-doped silica for improved hydrothermal stability and application to hydrogen separation membranes at high temperatures. *J Am Ceram Soc*. 2008;91:2975–2981.
27. Nomura M, Aida H, Gopalakrishnan S, Sugawara T, Nakao S, Yamazaki S, Inada T, Iwamoto Y. Steam stability of a silica membrane prepared by counterdiffusion chemical vapor deposition, *Desalination*. 2006;193:1–7.
28. Duke MC, da Costa JCD, Do DD, Gray PG, Lu GQ, Hydrothermally Robust Molecular Sieve Silica for Wet Gas Separation. *Adv Funct Mater*. 2006;16:1215–1220.
29. Sommer S, Klinkhammer B, Schleger M, Melin T. Performance efficiency of tubular inorganic membrane modules for pervaporation. *AIChE J*. 2005;51:162–177.

Manuscript received July 3, 2010, and revision received Sept. 9, 2010.